Echo-Induced Suppression of Coherent VLF Transmitter Signals in the Magnetosphere

R. RAGHURAM, T. F. BELL, R. A. HELLIWELL, AND J. P. KATSUFRAKIS

Radioscience Laboratory, Stanford University, Stanford, California 94305

Magnetospheric growth of coherent VLF signals transmitted from Siple Station, Antarctica, is inhibited by whistler mode echoes of earlier transmitter signals. This new phenomenon, called echo-induced suppression, is observed at least a third of the time that transmissions from Siple Station are detected at the receiving station in Roberval, Quebec, Canada. Suppression levels as high as 20 dB are observed. Though the echo is usually much weaker than the direct signal, the level of suppression is directly related to the amplitude of the echo. The echoes reduce the triggering of emissions as well as the growth of the signal. Echo-induced suppression is not explained by linear wave-wave interference. The echoes are thought to restrict growth by reducing the coherence of the total input signal. These new results suggest that coherent waves tend to limit their own growth even when particle distribution modification is unimportant. Other phenomena, such as whistler-induced suppression of signal growth, are thought to be related. Wave-induced growth suppression provides an indirect verification of the existence of discrete ducts for the propagation of VLF signals in the magnetosphere. It also provides a new tool for investigating wave-particle interactions in the magnetosphere.

INTRODUCTION

For more than 2 decades the whistler mode propagation of VLF waves along magnetic field lines in the magnetosphere has been studied. These waves may have their origin in lightning strokes (producing whistlers), man-made devices (e.g., VLF transmitters and power lines), or magnetospheric instabilities (e.g., VLF emissions). Their study has been based mainly on data received by ground stations [*Helliwell*, 1965]. Of special relevance here are several suppression effects associated with VLF emissions. For example, *Brice* [1964] showed that one set of periodic emissions often suppresses another. *Ho* [1973] reported that whistlers modify the period of quasi-periodic emissions and sometimes even terminate them. In general, when two VLF wave packets travel along the same path in the magnetosphere, one of the packets often suppresses the other. These and similar effects are considered important not only for understanding the generation of VLF emissions but also for providing a means of regulating wave growth in the magnetosphere. Their further study requires a controlled VLF signal source.

Controlled experiments on wave-particle interactions were started in 1973 by using a transmitter at Siple Station, Antarctica (84°W, 76°S) [*Helliwell and Katsufrakis*, 1974]. In this paper we describe a new magnetospheric suppression phenomenon observed during these experiments. It is found that the growth of transmitter signals is inhibited by the whistler mode echoes of earlier transmitter signals.

Figure 1 illustrates the propagation of VLF signals injected into the magnetosphere by the Siple transmitter (denoted by T). Some of the energy is trapped in a field-aligned magnetospheric duct and travels to the opposite hemisphere. The signals are received at Roberval, Quebec, Canada (denoted by R), which is magnetically conjugate to Siple Station. The waves pass through the wave-particle interaction region believed to be located close to the equator where amplification and triggering occur [*Helliwell*, 1967; *Helliwell and Crystal*, 1973; *Stiles and Helliwell*, 1977].

Figure 1 shows three 500-ms pulses separated in time by 1 s and traveling at roughly one-twentieth the velocity of light. The three pulses are shown at an instant in time. The pulse at A has not yet entered the interaction region and therefore shows no amplification. The pulse at C has already passed the interaction region. It grows in amplitude roughly exponentially during the first 200 ms, after which the amplitude saturates. The pulse undergoes temporal growth during the first 200 ms but only steady state spatial growth subsequently. The pulse at B, near the equator, shows both types of growth. From power change experiments it was found that the saturation amplitude increases with transmitter power.

The ducted waves are partially reflected at the base of the ionosphere near R and can return to the hemisphere from which they originated, where they may again be reflected. These reflected components are called echoes; the hop number of the echo is the number of times that the component has traveled through the magnetosphere. When a signal from Siple Station travels to Roberval, part of it is reflected and travels back to Siple Station, where it is again reflected. When such a reflected component or echo travels with a direct signal from the transmitter, the echo often inhibits the growth of the direct signal. This phenomenon will be referred to as echo-induced suppression.

A number of inferences can be drawn from the data on echo-induced suppression. The phenomenon provides a means of automatically regulating wave growth in the magnetosphere. The data are consistent with the theory that the observed propagation is ducted, as described by *Helliwell* [1965] and *Smith* [1960, 1961]. The suppression is not caused by simple linear wave-wave interference but is attributed to the effect of the echo on the wave-particle interaction process. It is postulated that growth suppression results from a reduction in the coherence of the total input signal, which is in turn caused by the emissions associated with the echoes. Whatever the explanation, it seems clear that a study of echo-induced suppression should lead to a more complete understanding of wave-particle interactions in the magnetosphere. It could, for example, explain the whistler-induced suppression of Siple transmitter signals [*Helliwell and Katsufrakis*, 1974], which appears to be governed by the same mechanism.

In the next section, particular examples of echo-induced suppression are described, while in the third section the important characteristics are presented. Echo-induced suppression is then interpreted, and the results are summarized.

Paper number 7A0248.

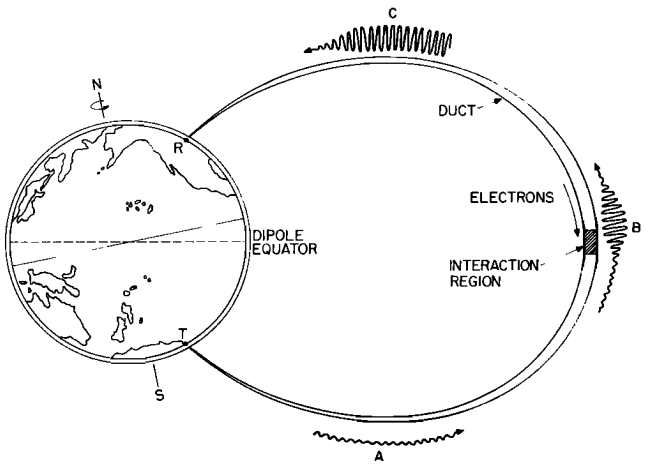

Fig. 1. Sketch showing propagation of transmitter signals between Siple Station and Roberval. Signals transmitted from Siple Station travel within a field-aligned duct of enhanced ionization. Amplification takes place in a wave-particle interaction region near the equator. Three 500-ms pulses at an instant in time are shown.

Examples of Echo-Induced Suppression

Echo-induced suppression is described here by using data from Roberval. Though the initial mixing between the direct signal and the echo takes place near Siple Station, they are both observed at Roberval only after they have traveled together through the magnetosphere once. Echo-induced suppression is manifested in different forms depending on the pulse sequence, as is illustrated in this section. In all cases, echo-induced suppression occurs during periods of overlap between the direct signals and three-hop echoes.

Figure 2 shows echo-induced suppression in 30-s pulses transmitted from Siple Station. Figure 2*c* shows the frequency-time spectrogram of a sample pulse, while Figure 2*d* shows the first few seconds of the pulse on an expanded time scale. Figure 2*a* shows the time sequence of a pulse and its echoes at both Siple Station and Roberval. On this day the travel time from Siple Station to Roberval at 5.15 kHz was 1.9 s, as is shown by the separation in time between successive hops or echoes. In Figure 2*d*, t_0 indicates the time of first arrival of the pulse at Roberval. The pulse grows in amplitude, and t_1 indicates the time at which the amplitude reaches saturation and the spectrum of the pulse begins to broaden. Such broadening is discussed in greater detail in the next section and is an important feature of the phenomenon. It takes 125 ± 50 ms for the amplitude to reach saturation; i.e., $t_1 - t_0 = 125$ ms. The initial growth rate on this day was 126 dB/s, and the total growth from noise level to saturation was 20 dB.

Figure 2*b* is a plot of the square of the amplitude versus time, averaged over 17 pulses received at Roberval. (The averaging helps to smooth out the effect of background noise, such as atmospherics.) A narrow band (260 Hz) centered at the transmitter frequency was digitally sampled, and the samples were averaged to produce the plot. There is a sharp drop in amplitude at t_2, which is 4.0 s after t_0. The spectrograms in Figures 2*c* and 2*d* show that the arrival of the three-hop echo also inhibits the triggering of emissions. The period of overlap between the three-hop echo and the direct signal, when echo-induced suppression occurs, is shown crosshatched in the time sequence. The times t_1 and t_0 are coincident in the time scale of Figure 2*b*.

If suppression were caused by the first arriving components of the echo, then the drop in amplitude should take place 3.8 s after the arrival of the one-hop, or direct, signal, about 200 ms ahead of the observed drop. The delay in the onset of suppression can be accounted for by the time taken for the spectrum to broaden. The time when three-hop echoes can be expected to have a broadened spectrum is given by $t_2 = t_1 + 3.8$ s. Within measurement accuracy (±50 ms) the onset of suppression is therefore coincident with the arrival of the spectrally broadened part of the three-hop echo.

Note that the three-hop echo itself is not discernable either in the spectrogram or in the averaged amplitude plot. Otherwise, there would be an extension in time of the signal beyond the termination of the direct signal. Three-hop echoes either are lost in the noise or are considerably weaker (<-20 dB) than the direct signal during periods of echo-induced suppression. When it is assumed that the echoes are weaker not only on the ground but also in the magnetosphere, they must affect the growth soon after entering the interaction region, where the echoes and unamplified signals probably are of comparable amplitude.

Suppression in Figure 2 is not uniform after t_2. Instead, there is a partial recovery in the amplitude 8.1 s from the start of the pulse. This is because the portion of the direct signal between 4.1 and 8.1 s is weaker and its subsequent echoes do not suppress as effectively. The level of suppression therefore depends on the amplitude of the echo. As a result, a variation in amplitude with roughly an 8-s period is seen over the entire length of the pulse. Though the suppression on this day was only 3.7 dB, it has been as high as 20 dB on other days. By using the whistler technique described by *Park* [1972] the path of propagation was located at $L = 4.2$.

An example of echo-induced suppression on two frequencies is shown in Figure 3. In the top panel is the frequency-time spectrogram showing a 31-s pulse and some shorter pulses on lower frequencies, all having been received at Roberval. The transmitter pattern, corrected for the one-hop travel time, is shown below the actual spectrum. The lower two panels are amplitude versus time plots of the received signal on two of the transmitted frequencies, 5.90 and 5.65 kHz. As is true in the example in Figure 2, suppression occurs after an initial two-hop whistler mode travel time in the 31-s pulse at 5.9 kHz. The signals on this day were multipath; i.e., they propagated along several paths with different travel times. There were two prominent paths with two-hop travel times of 3.7 s and 4.1 s, respectively. Here suppression begins at 3.9 s from the start of the pulse. This is about 200 ms after the first three-hop echo arrives at Roberval. This delay is equal to the time taken for the spectrum to broaden, as was explained in connection with Figure 2. There is again a partial recovery in the amplitude at 11 s UT. The alternating weak and strong segments can be seen over the entire length of the pulse. The direct pulse terminates at 33.05 s, and the frequency of transmission is changed to 5.65 kHz. The extension of the pulse seen in the spectrogram beyond 33.05 s at 5.9 kHz is caused by the three-hop echo, which is much weaker than the direct signal. As the bottom panel shows, transmissions at 5.65 kHz, beginning at 33.1 s, are not affected by echoes at 5.9 kHz. The pulse at 5.65 kHz also shows echo-induced suppression 4.2 s from the beginning of the pulse. The level of suppression for the pulse at 5.9 kHz was 15 dB, and the unsuppressed growth rate was 133 dB/s. The corresponding numbers at 5.65 kHz were 20 dB and 85 dB/s.

A different form of echo-induced suppression is manifested in Figure 4. At the top is a time sequence of 3.45-kHz pulses as

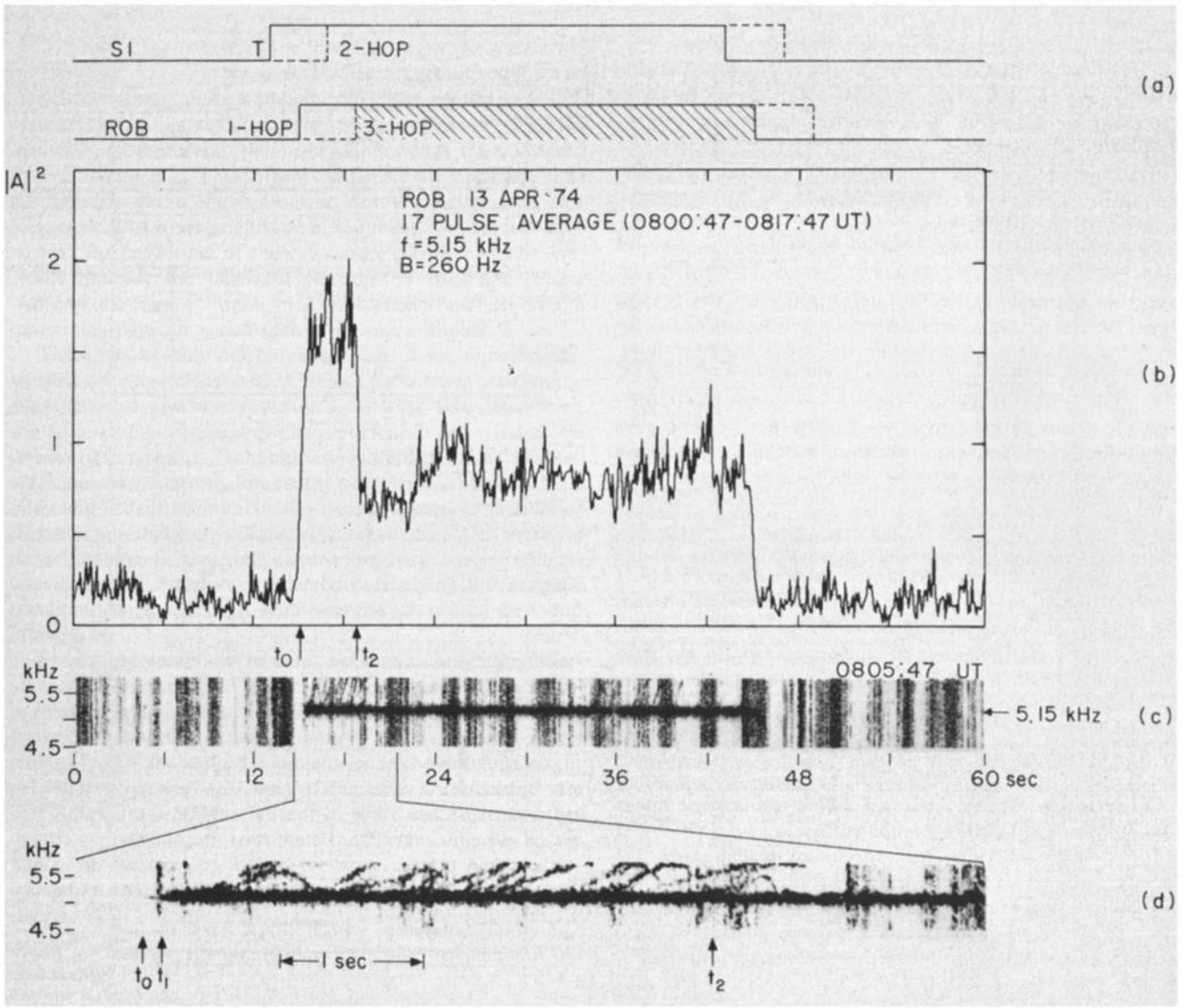

Fig. 2. Variation in amplitude of 30-s pulses received at Roberval. (*a*) Time sequence of the various hops. (*b*) Square of the amplitude as a function of time. The plot is a 17-pulse average. Echo-induced suppression is seen in the form of a reduction in amplitude 4.0 s from the start of the pulse. (*c*) Frequency-time spectrogram of a typical pulse from this time interval. (*d*) Spectrogram showing the first few seconds on an expanded time scale. Echo-induced suppression is again clearly seen in the spectrograms. See text for an explanation of t_0, t_1, and t_2.

received at Roberval. The solid lines represent the direct signal, the dashed lines the three-hop echo, and the crosshatched area the period of overlap when suppression can be expected to occur. The two-hop travel time is denoted by τ. Below the time sequence is the observed spectrogram. At the bottom is a plot of the amplitude in a 150-Hz-wide passband centered on the carrier. Two-second pulses were transmitted with varying time intervals between them. (During these intervals there were transmissions at 2.45 and 2.65 kHz; they were barely detectable at Roberval and are not of interest here.) The three-hop echoes of the 2-s pulses are weak but are seen clearly in both the spectrogram and the amplitude plot. The first half of the last direct pulse starting at 24.5 s shows echo-induced suppression. In Figures 2 and 3 the received pulses were initially stronger. Here, in Figure 4, the opposite effect is seen; the initial part of the pulse is weaker. Even at the end of the echo this pulse does not reach the amplitude of the earlier direct pulses. Here again, the presence of the three-hop echo inhibits not only the growth of the signal but also the triggering of emissions. For this case the level of suppression was 9.5 dB, and the growth rate 98 dB/s.

Another example of echo-induced suppression, similar to that in Figure 4, is shown in Figure 5. The spectrum and the narrow-band amplitude are shown in the middle and lower panels, respectively. Two-second pulses were transmitted with 2-s intervals between them, as is shown by the sketch in the top panel. Here the first parts of four pulses received at Roberval are seen to be relatively weaker. The two-hop whistler mode travel time τ was 2.9 s, so that the three-hop echo of the latter half of each pulse arrived with the direct signal of the next pulse. In this figure, as in Figure 4, the crosshatched regions in the top panel represent times of overlap, when echo-induced suppression takes place. Each of the arrows along the time scale indicates the time at which the amplitude starts to recover after the termination of the echo. The termination of the corresponding direct pulse can be seen τ s before each arrow except the first. Note that the emissions at the end of the pulses increase their apparent length. (The thin lines at 6060 and 5340

Hz on the spectrogram are caused by induction fields at harmonics of 60 Hz from the Canadian power system.) As occurs in the example in Figure 2, the echoes affect the triggering as well as the amplification. The level of suppression was more than 13 dB on some pulses on this day. The path of propagation calculated from whistler measurements was $L = 3.7$. The growth rate during the times of recovery at the end of suppression was about 110 dB/s.

At first sight it might seem that echo-induced suppression could be explained by linear wave-wave interference. However, the repetition of the phenomenon in every pulse, as in Figure 5, makes this interpretation unlikely. Radial drifts of the ducts usually cause changes in path length of the order of a wavelength per second [*Carpenter and Seely*, 1976; *McNeill*, 1967]. One would therefore expect to see constructive interference as often as destructive interference. Since constructive wave interference has not been observed, linear wave-wave interference as a cause of echo-induced suppression can be ruled out.

Characteristics of Echo-Induced Suppression

The features of echo-induced suppression that are obvious from the data were described in the last section. Some other features are described here.

The phenomenon is relatively frequent, and the features are repeatable. In 7 months (April 2 to November 1) of transmissions in 1974, echo-induced suppression was observed on a third of the days that transmitter signals were detected at Roberval. (This frequency of occurrence represents a lower bound because the transmitted program is quite often not suitable for the detection of this phenomenon.) Echo-induced suppression is always accompanied by temporal growth and quite often by triggering.

The path of propagation was estimated on 18 days during periods of echo-induced suppression to determine if the phenomenon was restricted to any range of L values. The paths were calculated from the nose frequencies of whistlers which had the same travel times as the transmitter signals [*Park*, 1972; *Carpenter and Miller*, 1976]. The paths ranged from $L = 3.5$ to $L = 5$. The distribution was similar to the more complete histogram shown by *Carpenter and Miller* [1976] for transmitter signals observed at Roberval. Echo-induced suppression tends to occur during periods of magnetospheric quieting following a moderate disturbance. *Carpenter and Miller* [1976] observed similar behavior in the occurrence of transmitter signals at Roberval. Thus the conditions under which echo-induced suppression occurs are similar to those for the observation of transmitter signals at Roberval, and no further special conditions are necessary.

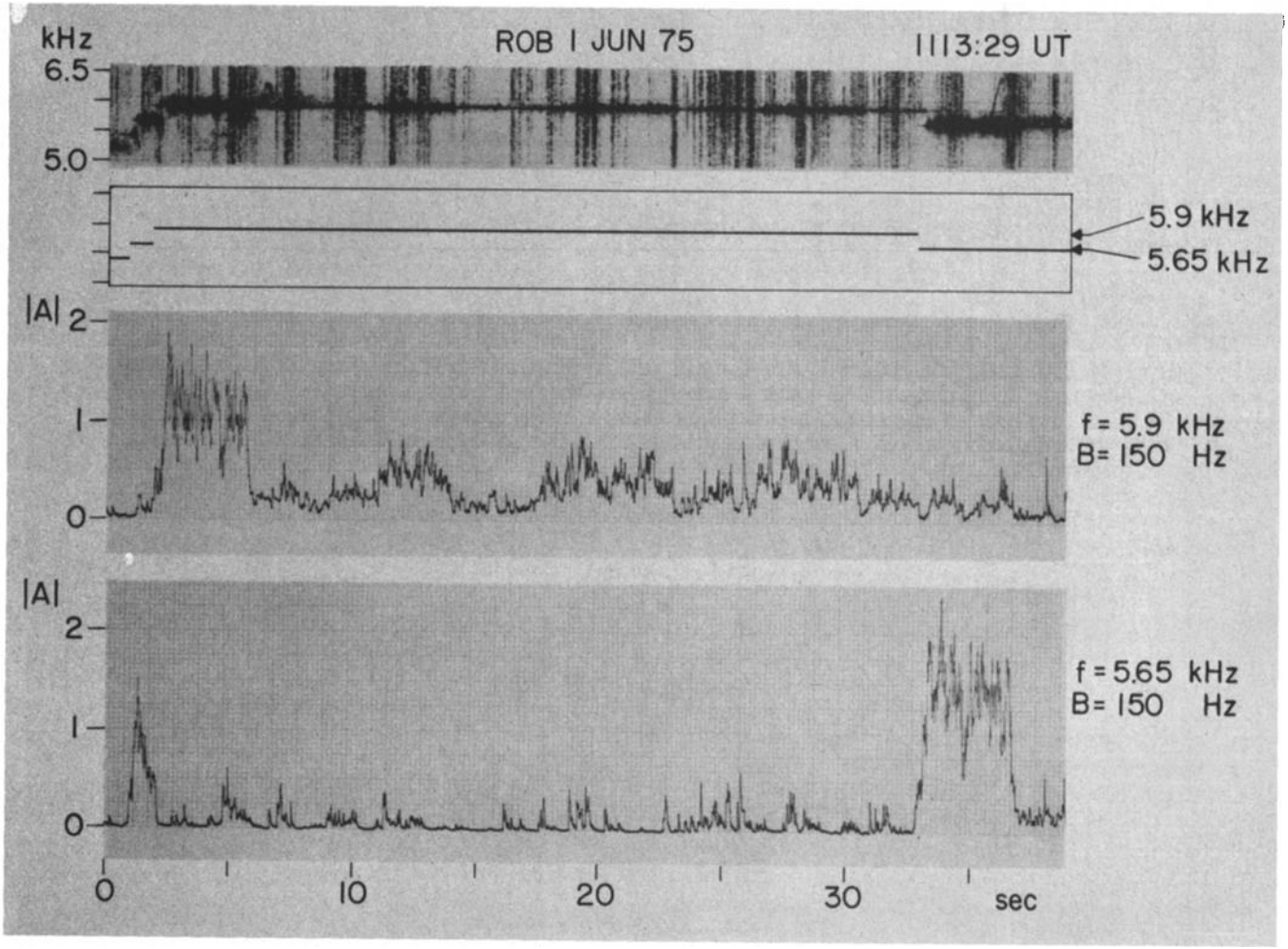

Fig. 3. Echo-induced suppression seen in a 31-s pulse transmitted at 5.9 kHz. The top panel shows the frequency-time spectrogram with the transmitter format below it. The lower two panels show amplitude versus time. The amplitude data were obtained by passing the signal through 150-Hz filters centered at 5.9 kHz and 5.65 kHz, respectively. The three-hop echoes of the 1-s pulses at the beginning as well as that of the 31-s pulse are visible.

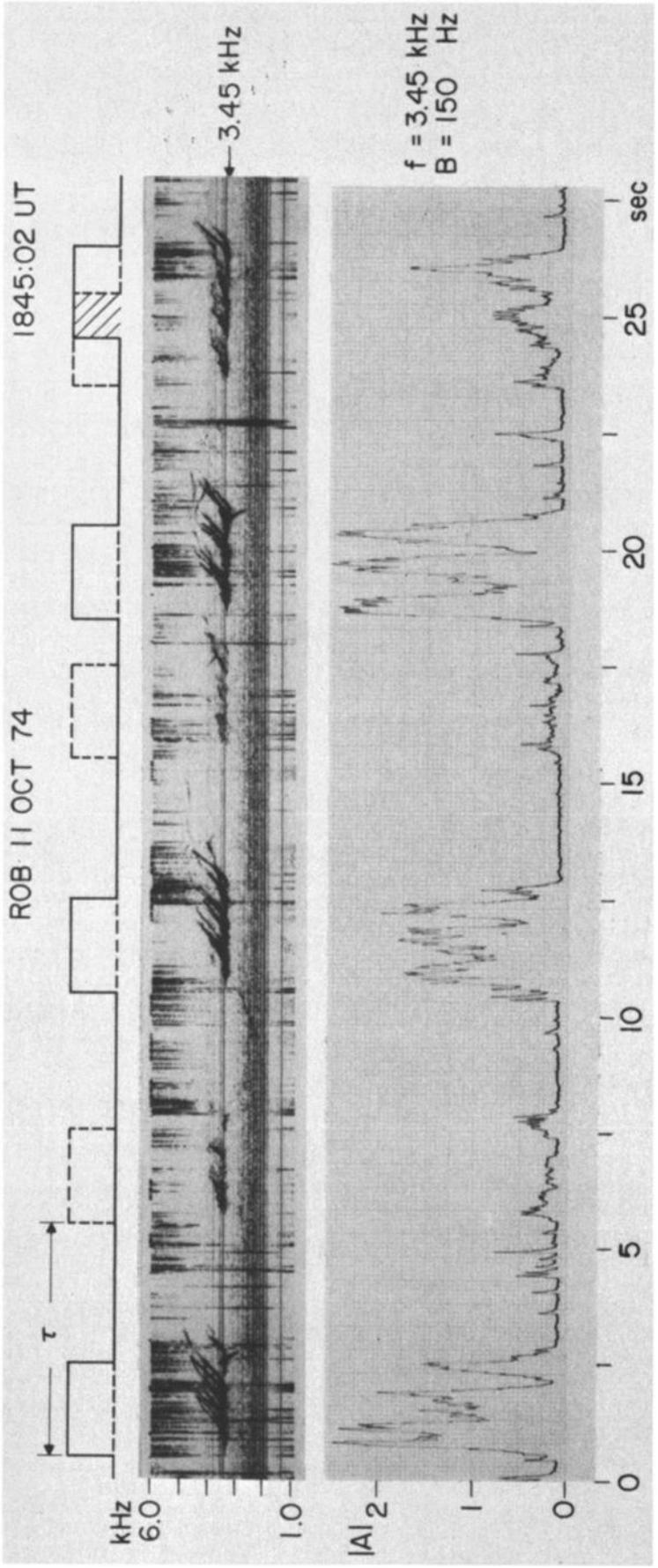

Fig. 4. Two-second pulses separated by varying time intervals. The timing sequence at the top shows the direct signal by solid lines and the three-hop echoes by dashed lines. The crosshatched region represents the period of overlap when echo-induced suppression can be expected to occur. The two-hop whistler mode delay τ is 5 s. Echo-induced suppression is seen in the last pulse in both the spectrogram and the amplitude plot. The amplitude plot was obtained by using a 150-Hz filter centered at the transmitter frequency, as was done in Figure 3. Note that the amplitude of the echoes is far weaker than that of the direct signals.

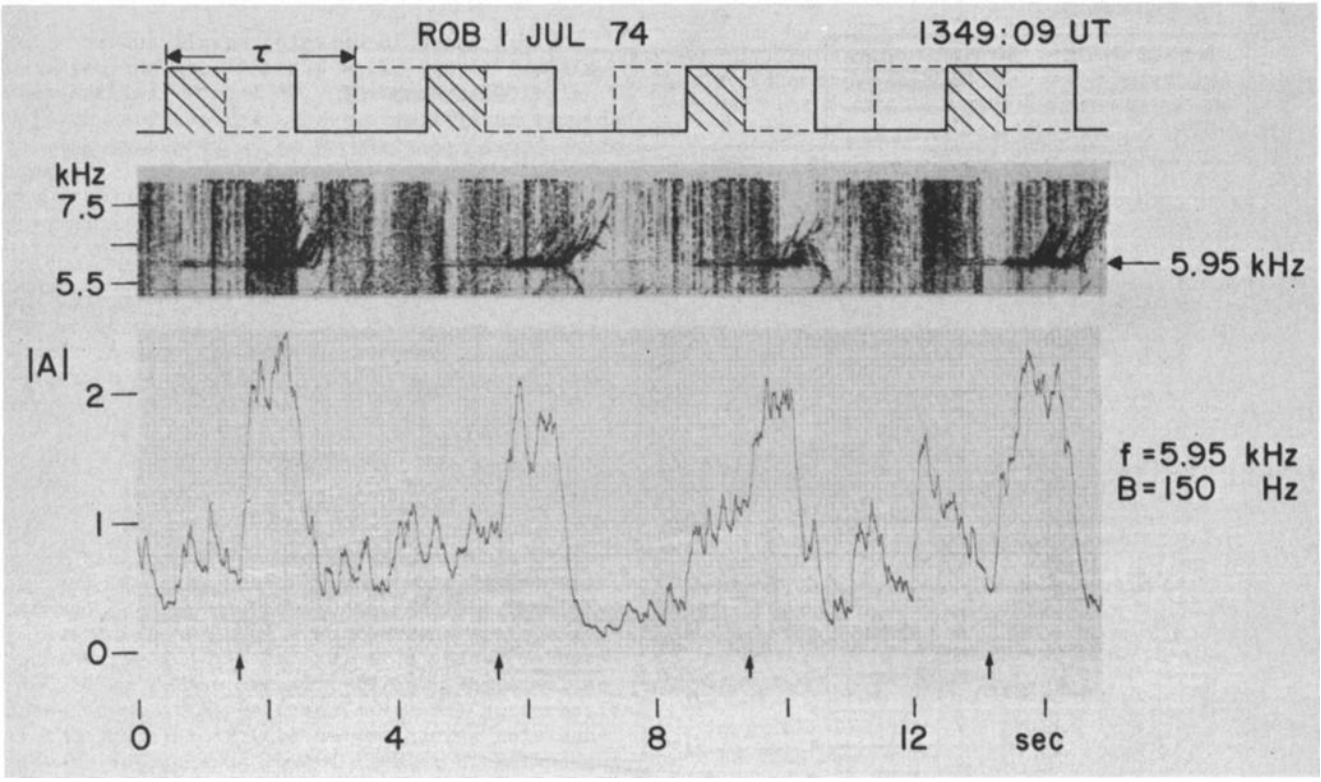

Fig. 5. Two-second pulses, spaced 2 s apart, showing echo suppression. Here, as in Figure 4, the periods of overlap which correspond to periods of echo-induced suppression are shown crosshatched. The arrows mark the start of the recovery in amplitude.

A feature of echo-induced suppression, which was suggested by several of the spectrograms in the last section, is that the signals received at Roberval have bandwidths as high as 150 Hz. A monochromatic input generates these additional frequencies mainly on the higher side, as is illustrated in Figure 6. The case analyzed here is the 31-s pulse shown in Figure 3. The data were sampled and transformed by using a fast Fourier transform routine similar to that described by *Stiles and Helliwell* [1975]. The time segments were 0.64 s long, there being an overlap of 0.32 s between successive transforms. Thus a separate transform was obtained every 0.32 s, alternate transforms being completely independent. Each A-scan is an average over 13 such transforms. The A-scan on the left is an average over the first 4.16 s of the pulse, when there was no suppression. The transmitter frequency is shown by the arrow. The bandwidth is almost 100 Hz, the amplitude decaying at higher frequencies. Also, the additional frequencies are predominantly above the transmitter frequency. Usually, the three-hop echoes also contain these additional frequencies. Sometimes, only the additional frequencies above the transmitter frequency are present in the three-hop echo, the transmitter frequency itself being below the noise level. The A-scan on the right is an average over the next 4.16 s, when the signal was suppressed. Not only is the amplitude at the transmitter frequency reduced, but so is the bandwidth.

From evidence such as that in Figure 6 it was hypothesized that an echo of finite bandwidth would be able to suppress a direct input signal anywhere within its band. To test this proposition, successive transmitted pulses were stepped up in frequency by Δf. The results as received at Roberval are shown in Figure 7. The transmitted format is shown in the bottom panel. The pulses are separated by varying intervals of time. The sequence begins with a 10-s pulse at 5.4 kHz. The Δf steps in the five data panels are 100, 0, 10, 25, and 50 Hz. Note that the three-hop echoes of most of the pulses are seen clearly, for example, at 13 s and 21 s. The variations in amplitude of the three-hop echoes of the 10-s pulses (near 12 s) reflect variations in the direct signal caused by echo-induced suppression. The two-hop time delay for the various propagation paths varied

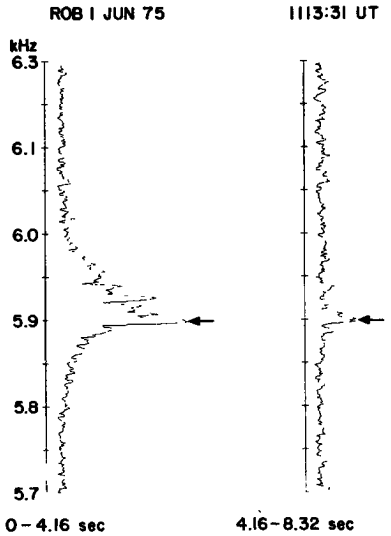

Fig. 6. Integrated amplitude versus frequency (A-scans) showing echo-induced suppression. Each A-scan is an average of 13 separate scans in frequency. The left A-scan shows the unsuppressed signal, and the right shows the suppressed signal. The case analyzed here is the 31-s pulse shown in Figure 3. During periods of echo-induced suppression, both the transmitter frequency and the upper side band are suppressed. Note that in the absence of echoes the received signal at Roberval has a bandwidth of more than 100 Hz.

from 3 to 4.8 s. However, the delay for the most prominent path was 4.4 s, so that the three-hop echo of the third pulse arrived near 26 s, at roughly the same time (0.4 s later) as the fourth pulse, suppressing its growth. The bandwidth of these signals is typically more than 100 Hz, thus providing a sufficient spread in the echoing components to account for suppression at each value of Δf. The fourth pulse is suppressed for all values of Δf, although the spectrogram does not show this very convincingly. Amplitude recordings (not shown) gave a measured suppression for the fourth pulse of about 9 dB. Although there is growth, the triggering on this day (see also Figures 3 and 8) is less than that in Figures 2, 4, and 5. This

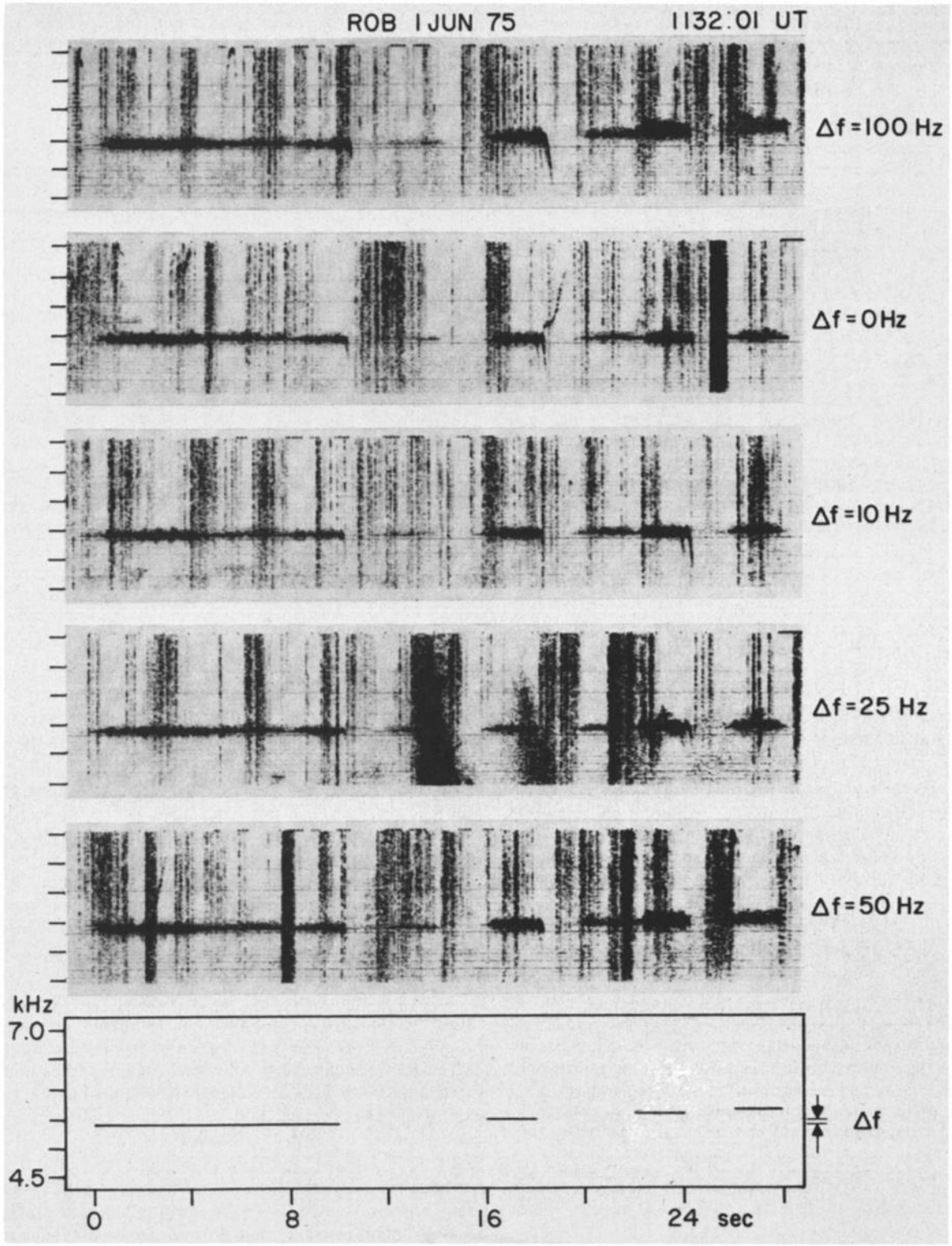

Fig. 7. Echo-induced suppression when successive pulses are stepped up in frequency. The transmitter program is shown in the bottom panel, the time scale being corrected to allow for the one-hop travel time. The parameter Δf is varied as shown. The last pulse is weaker because of echo-induced suppression for all values of Δf. Three-hop echoes are clearly visible on these spectrograms.

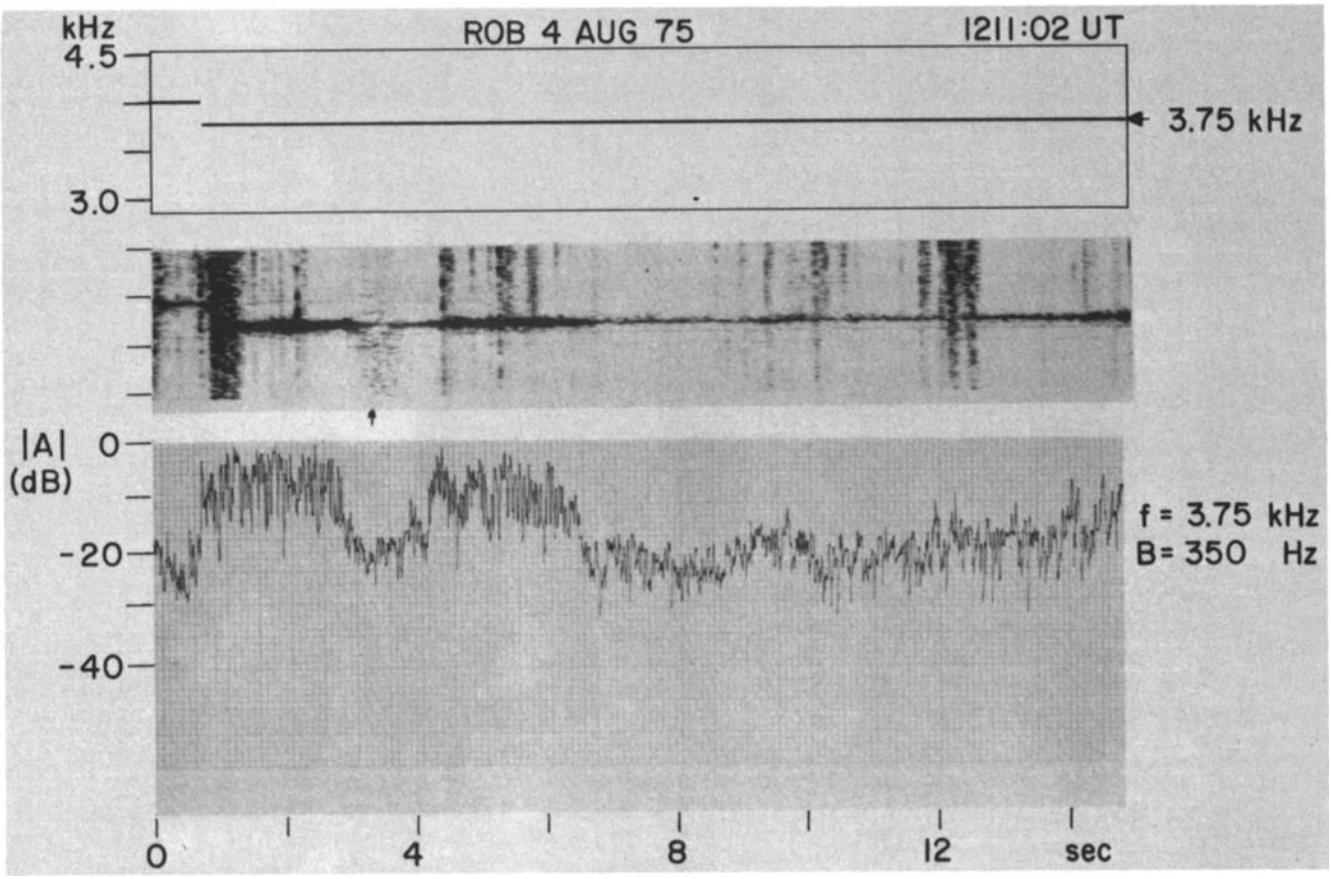

Fig. 8. Whistler-induced suppression and echo-induced suppression are seen to occur together. The top panel shows the transmitter program corrected for the one-hop travel time. Both the spectrogram and the amplitude plot show suppression caused by a diffuse whistler between 3 and 4 s, marked by an arrow. Echo-induced suppression occurs at 6.6 s. The partial recovery at 9 s is related to the whistler-induced suppression, and the two events are separated by the two-hop travel time.

may be caused by the multihop echoes of earlier transmissions (below the threshold of detection here) suppressing the emissions rising in frequency.

The suppression of transmitter signals by whistlers reported earlier by *Helliwell and Katsufrakis* [1974] bears a strong resemblance to echo-induced suppression. The two effects often occur together, and the mechanism of growth inhibition appears to be the same. Figure 8 shows a long pulse at 3.75 kHz displaying both effects. The upper panel shows the transmitter format as it would be seen at Roberval, the middle panel shows the spectrum at Roberval, and the bottom panel shows an amplitude plot on a decibel scale. The drop in amplitude at 6.6 s is due to echo-induced suppression, while that from 3 to 4.2 s is due to whistler-induced suppression. The whistler indicated by an arrow can be seen clearly, though faintly, in the spectrogram. Because of path mixing, the whistler has the appearance of a diffuse noise burst, lasting about 1 s, instead of a discrete trace. The three-hop echo of the portion of signal between 3 and 4.2 s is weaker and does not suppress as effectively. This accounts for the partial recovery in signal amplitude at 9 s. The two suppression effects are often observed together, as they are in this case, and appear to be governed by the same mechanism, the diffuse whistlers playing the role of the transmitter signal echo.

Discussion of Results

The key to an explanation of echo-induced suppression is thought to be the stimulation of new frequency components by the monochromatic transmitted pulse. Before outlining a suppression mechanism, one must identify a mechanism for amplifying VLF waves in the magnetosphere. It is generally accepted that the mechanism depends on Doppler-shifted cyclotron resonance between electrons and waves. Often, the linear theory of plasma instability is used to predict growth [e.g., *Kennel and Petschek,* 1966; *Liemohn,* 1967]. An imaginary frequency or wave number is calculated from the dispersion relation. Such an approach is not suitable here. In the linear theory the presence of additional components at other frequencies would not affect the growth of the transmitter signal. The different frequency waves would grow independently, and there would be beating but no reduction in amplitude.

Instead, a nonlinear theory is considered. One class of nonlinear theories [*Brice,* 1964; *Helliwell,* 1967; *Helliwell and Crystal,* 1973; *Dysthe,* 1971; *Nunn,* 1974] employs phase-bunched currents to explain VLF emissions and amplification. The bunching is produced by the perturbation of the parallel velocities of the electrons by the $q(v_\perp \times B_w)$ force, where q is the charge on the electron, $v_\perp$ the perpendicular velocity of the electron, and B_w the wave magnetic field. The time required for bunching to occur varies inversely with the square root of the amplitude of the wave. A wave has a coherence time roughly equal to the reciprocal of its bandwidth. (The nature of the spectrum should be taken into account for a more exact calculation.) If τ_C is the coherence time and τ_B is the phase-bunching time, then the amplification will be either partially or totally suppressed when $\tau_C < \tau_B$.

For example, the pulse analyzed in Figure 6 would have a

coherence time of about 10 ms. A 1-mγ wave for conditions typical at $L = 3$ has a phase-bunching time of approximately 20 ms [*Helliwell and Crystal*, 1973]. It should be remembered that for sufficiently strong fields, significant phase bunching will take place even after the initial bunching period has passed. Therefore whenever the coherence time is less than the total interaction time, some suppression can be expected. The length of the interaction region may therefore be an important factor in addition to the wave amplitude and bandwidth.

There is obviously a maximum separation in frequency between the direct signal and the echo for which suppression occurs. This frequency difference is defined as the interaction bandwidth. For example, in Figure 3, direct signals at 5.65 kHz are apparently unaffected by three-hop echoes at 5.9 kHz. Therefore the interaction bandwidth must be less than 250 Hz for this case. This bandwidth depends on the amplitude and frequency of the wave, the magnetospheric parameters, and the pitch angle of the particles involved.

Assuming phase bunching to be the controlling mechanism, we can estimate the interaction bandwidth within which an interfering wave at f_2 can significantly affect the growth of another wave at f_1. If the interfering wave can phase-bunch electrons that are resonant at f_1, then these electrons will not be available for growth at f_1. Thus the bunching time, which is one quarter of the small-amplitude trapping period [*Crystal*, 1975; *Brinca*, 1972], must be less than, say, one half of the period of the beat between the two frequencies. This means that the interaction bandwidth is twice the small-amplitude trapping frequency. At $L = 3$ for a 30° pitch angle electron and a 1-mγ wave at half the gyrofrequency this trapping frequency is 16 Hz. Roughly speaking, a transmitter signal could be suppressed by echoes having components within 32 Hz of the transmitter frequency. Again roughly speaking, suppression should be less for frequency deviations either greater or less than 32 Hz.

It is our intention here only to outline a mechanism for echo-induced suppression and to point out the relevant quantities linked to an explanation. A more detailed explanation requires consideration of signals of finite bandwidth interacting with electrons in a nonlinear fashion.

Echo-induced suppression is a natural means of regulating the growth process in the magnetosphere. If the amplification increases, the echoes get stronger and thereby reduce the amplification. In addition, the amplitude of the echoes is regulated whatever the conditions for echoing are. At times of relatively good echoing, the growth of the direct signal is suppressed, and the amplitude of the echoes is thereby decreased. When echoing conditions are poor, there is less suppression and hence increased amplification of the direct signal. Echo-induced suppression therefore provides a form of automatic gain control for narrow-band VLF waves in the magnetosphere. It is interesting to compare this finding with the predictions of the quasi-linear theory described by *Kennel and Petschek* [1966] in connection with natural VLF broadband hiss. In their model the output signal increases with increased reflection coefficient. They therefore require a consequent reduction in trapped particle flux to limit wave growth. Echo-induced suppression, on the other hand, suggests that waves can limit their own growth as a result of the echoing process and that modification of particle fluxes need not be invoked.

Echo-induced suppression can take place only if the three-hop echo and the direct signal are traveling along the same path or closely adjacent paths. This is consistent with the model for ducted propagation of *Helliwell* [1965] (see also *Smith* [1960, 1961]).

Summary of Results

A new magnetospheric wave-particle interaction phenomenon called echo-induced suppression has been described. Whistler mode echoes of VLF transmitter signals are observed to suppress the growth of the direct signals. The important characteristics and some of the implications of this echo-induced suppression are summarized below.

1. Echo-induced suppression is a relatively frequent phenomenon. It occurs on at least a third of the days on which transmitter signals are detected at Roberval.

2. The suppression is not due to linear wave-wave interference. This is evident from the consistent suppression in every pulse, as shown in Figure 5. The explanation is related to the nonlinear wave-particle interaction process.

3. Echo-induced suppression must occur at the input to the amplification region, where the echo and the direct signal are expected to have comparable amplitudes.

4. During periods of echo-induced suppression, any unsuppressed first-hop signals and their echoes show spectral broadening at frequencies predominantly above the transmitter frequency. The broadband nature of the echo reduces the coherence of the direct signal, thereby reducing its growth. Linear plasma instability theories do not predict echo-induced suppression. Nonlinear models of wave growth [*Helliwell and Crystal*, 1973; *Nunn*, 1974; *Dysthe*, 1971; *Brinca*, 1972] require a transient period corresponding to the phase-bunching time of *Helliwell and Crystal* [1973]. This suggests that echo-induced suppression occurs when the wave coherence time is less than the phase-bunching time.

5. Echo-induced suppression indicates that waves undergoing nonlinear amplification in the magnetosphere can regulate their own growth through the echoing process.

6. Echo-induced suppression is consistent with the ducting model of *Helliwell* [1965].

In short, echo-induced suppression is fundamental to an understanding of wave-particle interactions in the magnetosphere; other phenomena, such as whistler-induced suppression, appear to be related. Echo-induced suppression may even play a role in VLF communications. For example, it could be used selectively to suppress the magnetospheric component by equating the time between pulses to the two-hop travel time. For magnetospheric studies, suppression can be avoided by preventing overlaps of the direct signal and the echo. Echo-induced suppression also brings out the importance of controlled VLF signals for magnetospheric studies, since it probably would not have been discovered by other means.

Acknowledgments. The authors' work was supported in part by the Division of Polar Programs of the National Science Foundation under grant OPP-04093, in part by the Atmospheric Sciences Section of the National Science Foundation under grant ATMO7707, and in part by the Office of Naval Research under contract N00014-76-C-0689. Special thanks are due Holmes and Narver, Inc., Anaheim, California, and the Department of Defense for the logistic support of Siple Station, Antarctica.

The Editor thanks K. Maeda and L. R. O. Storey for their assistance in evaluating this paper.

References

Brice, N. M., Discrete VLF emissions from the upper atmosphere, *Tech. Rep. SEL64-088*, Radioscience Lab., Stanford Electron. Lab., Stanford Univ., Stanford, Calif., 1964.

Brinca, A. L., A whistler side-band growth due to nonlinear wave-particle interaction, *J. Geophys. Res.*, *77*, 3508, 1972.

Carpenter, D. L., and T. R. Miller, Ducted magnetospheric propagation of signals from the Siple, Antarctica, VLF transmitter, *J. Geophys. Res.*, *81*, 2692, 1976.

Carpenter, D. L., and N. Seely, Cross-*L* drifts in the outer plasmasphere: Quiet time patterns and some substorm effects, *J. Geophys. Res., 81,* 2728, 1976.

Crystal, T. L., Nonlinear currents stimulated by monochromatic whistler-mode waves in the magnetosphere, *Tech. Rep. SEL3465-4,* Radioscience Lab., Stanford Electron. Lab., Stanford Univ., Stanford, Calif., 1975.

Dysthe, K. B., Some studies of triggered whistler emissions, *J. Geophys. Res., 76,* 6915, 1971.

Helliwell, R. A., *Whistlers and Related Ionospheric Phenomena,* Stanford University Press, Stanford, Calif., 1965.

Helliwell, R. A., A theory of discrete VLF emissions from the magnetosphere, *J. Geophys. Res., 72,* 4773, 1967.

Helliwell, R. A., and T. L. Crystal, A feedback model of cyclotron interaction between whistler mode waves and energetic electrons in the magnetosphere, *J. Geophys. Res., 78,* 7357, 1973.

Helliwell, R. A., and J. P. Katsufrakis, VLF wave injection into the magnetosphere from Siple Station, Antarctica, *J. Geophys. Res., 79,* 2511, 1974.

Ho, D., Interaction between whistlers and quasi-periodic VLF emissions, *J. Geophys. Res., 78,* 7347, 1973.

Kennel, C. F., and H. E. Petschek, Limit on stably trapped particle fluxes, *J. Geophys. Res., 71,* 1, 1966.

Liemohn, H. B., Cyclotron resonance amplification of VLF and ULF whistlers, *J. Geophys. Res., 72,* 39, 1967.

McNeill, F. A., Frequency shifts on whistler mode signals from a stabilized VLF transmitter, *Radio Sci., 2,* 589, 1967.

Nunn, D., A self-consistent theory of triggered VLF emissions, *Planet. Space Sci., 22,* 349, 1974.

Park, C. G., Methods of determining electron concentrations in the magnetosphere from nose whistlers, *Tech. Rep. 3454-1,* Radioscience Lab., Stanford Electron. Lab., Stanford Univ., Stanford, Calif., 1972.

Smith, R. L., Guiding of whistlers in a homogeneous medium, *J. Res. Nat. Bur. Stand., Sect. D, 64,* 505, 1960.

Smith, R. L., Propagation characteristics of whistlers trapped in field-aligned columns of enhanced ionization, *J. Geophys. Res., 66,* 3699, 1961.

Stiles, G. S., and R. A. Helliwell, Frequency-time behavior of artificially stimulated VLF emissions, *J. Geophys. Res., 80,* 608, 1975.

Stiles, G. S., and R. A. Helliwell, Stimulated growth of coherent VLF waves in the magnetosphere, *J. Geophys. Res., 82,* 523, 1977.

(Received November 8, 1976;
accepted March 10, 1977.)